Neoplasia • Vol. 8, No. 5, May 2006, pp. 419–428 419

www.neoplasia.com

Sustained Angiopoietin-2 Expression Disrupts Vessel Formation and Inhibits Glioma Growth[1]

Ok-Hee Lee, Juan Fueyo*, Jing Xu*, W. K. Alfred Yung*, Michael G. Lemoine*, Frederick F. Lang†, B. Nebiyou Bekele‡, Xian Zhou‡, Marta A. Alonso*, Kenneth D. Aldape§, Gregory N. Fuller§ and Candelaria Gomez-Manzano**

Departments of *Neuro-Oncology, †Neurosurgery, ‡Biostatistics, and §Pathology, The University of Texas M. D. Anderson Cancer Center, Houston, TX, USA

Abstract

Systematic analyses of the expression of angiogenic regulators in cancer models should yield useful information for the development of novel therapies for malignant gliomas. In this study, we analyzed tumor growth, vascularization, and angiopoietin-2 (Ang2) expression during the development of U-87 MG xenografts. We found that tumoral angiogenesis in this model follows a multistage process characterized by avascular, prolific peripheral angiogenesis, and late vascular phases. On day 4, we observed an area of central necrosis, a peripheral ring of Ang2-positive glioma cells, and reactive Ang2-positive vascular structures in the tumor/brain interface. When the tumor had developed a vascular network, Ang2 was expressed only in peripheral vascular structures. Because Ang2 expression was downmodulated in the late stages of development, probably to maintain a stable tumoral vasculature, we next studied whether sustained Ang2 expression might impair vascular development and, ultimately, tumor growth. Ang2 prevented the formation of capillary-like structures and impaired angiogenesis in a chorioallantoic membrane chicken model. Finally, we tested the effect of sustained Ang2 expression on U-87 MG xenograft development. Ang2 significantly prolonged the survival of intracranial U-87 MG tumor–bearing animals. Examination of Ang2-treated xenografts revealed areas of tumor necrosis and vascular damage. We therefore conclude that deregulated Ang2 expression during gliomagenesis hindered successful angiogenesis and that therapies that sustain Ang2 expression might be effective against malignant gliomas.

Neoplasia (2006) **8,** 419–428

Keywords: Glioma, animal model, vascular development, tumor growth, angiopoietin-2.

Introduction

Malignant gliomas, the most common subtype of primary brain tumor, are aggressive and neurologically destructive. Poor outcome is best exemplified by a median survival of 9 to 12 months in patients with glioblastoma multiforme (GBM), the most aggressive form of glioma, despite maximum treatment efforts [1]. More effective treatments for these tumors now depend almost entirely on a better understanding of the biology of these tumors. Thus, by delineating the molecular events that occur during glioma formation, researchers should be able to design therapies that target the multistage nature of tumorigenesis.

One of the major pathophysiologic characteristics of malignant gliomas—indeed of solid tumors in general—is their ability to induce a robust angiogenic response, with GBMs being one of the most vascularized tumors in humans [2]. If neovascularization is prevented, tumor growth is dramatically impaired, with the tumor volume restricted to a few cubic millimeters [3]. Thus, agents that inhibit angiogenesis are particularly attractive as a therapeutic option [4,5].

Animal models of cancer, including both traditional tumor transplant models and newer genetically engineered mouse models of cancer, have helped establish the causality of angiogenesis [6–8] and have provided the means for assessing antiangiogenic therapeutic strategies [6,9,10]. Implantation of U-87 MG glioma cells into immunodeficient animals produces solid intracerebral tumors, and the growth characteristics of these tumors are reproducible. For such reason, U-87 MG is one of the most frequently used models for testing therapies for malignant gliomas [11]. However, comparatively little is known about the chronology of angiogenesis in this model. In this study, we therefore first characterized the tumor growth and vascular development of the human glioma xenograft U-87 MG in a nude mouse model. In particular, we focused on angiopoietin-2 (Ang2) because of descriptive studies suggesting that

Abbreviations: Ang2, angiopoietin-2; GBM, glioblastoma multiforme; VEGF, vascular endothelial growth factor; HUVEC, human umbilical vein endothelial cell; MOI, multiplicity of infection; PCNA, proliferating cell nuclear antigen; SMA, smooth muscle actin; MVD, microvessel density; CAM, chorioallantoic membrane; SD, standard deviation

Address all correspondence to: Candelaria Gomez-Manzano, MD, Department of Neuro-Oncology, The University of Texas M. D. Anderson Cancer Center, Box 1002, 1515 Holcombe Boulevard, Houston, TX 77030. E-mail: cmanzano@mdanderson.org

[1]This work was supported by the National Institutes of Health (W.K.A.Y.), an institutional research grant from the M. D. Anderson Cancer Center (C.G.M.), the Brain Tumor Research Trust (W.K.A.Y.), and National Cancer Institute Cancer Center Support Grant CA-16672 (M. D. Anderson Cancer Center).

DOI 10.1593/neo.06109

it is a complex regulator of vascular remodeling that plays a role in both vessel sprouting and vessel regression. This concept of Ang2 as a destabilizing signal that causes vessels to revert to a more plastic and tenuous state, which was initially formulated based on observations in ovary remodeling [12,13], is consistent with more recent data obtained from transgenic mice [14]. In addition, in gliomas, Ang2 expression has been detected in coopted tumor vessels and in areas of vessel regression during angiogenesis [7,8]. However, the function of Ang2 in glioma angiogenesis is still not certain [15,16]. Based on observed spatial and temporal expression patterns of Ang2, we then hypothesized that sustained Ang2 expression could lead to impaired vascularization and, ultimately, to impaired tumor growth. We thus also tested the sustained expression of Ang2 in a U-87 MG tumor–bearing nude mouse model.

Materials and Methods

Cell Lines and Culture Conditions

U-87 MG cells were obtained from the American Type Culture Collection (Manassas, VA) and maintained in Dulbecco's modified Eagle's/F12 medium (1:1 vol/vol) supplemented with 10% fetal bovine serum in a humidified atmosphere containing 5% CO_2 at 37°C. Human umbilical vein endothelial cells (HUVECs; passages 2–7) were maintained as recommended by the manufacturer (Clonetics, Walkersville, MD).

Animal Studies

To study tumor growth and the angiogenic pattern of U-87 MG xenografts, 5×10^5 U-87 MG cells were engrafted into the caudate nuclei of athymic mice (4- to 6-week-old female mice; Harlan-Sprague Dawley, Inc., Indianapolis, IN) using a previously described guide-screw system [17]. Engrafted animals were sacrificed 8 hours and 1, 4, 6, 12, 17, and 20 days after cell implantation ($n = 3–4$ per time point). The animals were anesthetized before sacrifice; sacrifice was performed by perfusing their hearts with 4% paraformaldehyde. The brains were incubated overnight in 4% paraformaldehyde and then embedded in paraffin. The brains were sectioned along the coronal plane to identify detectable tumors and to prepare specimens for microscopic examination. Hematoxylin and eosin (H&E)–stained slides were evaluated to look for evidence of tumors and to identify the characteristics of tumors. The largest (a) and smallest (b) diameters of the tumors were measured, and tumor volume was calculated using the formula: $0.4ab^2$ [18].

To assess the anticancer effects of Ang2, U-87 MG cells (5×10^5) were implanted in murine brains, and AdCMV, AdAng2, or vehicle [phosphate-buffered saline (PBS)] was administered locally (1.5×10^8 pfu) starting 3 days later and continuing twice weekly for 3 weeks. Thus, animals were treated with intratumoral injections of AdAng2, AdCMV, or PBS starting on day 4 after cell implantation. Animals showing generalized or localized symptoms of toxicity were sacrificed. Surviving animals were sacrificed 115 days after cell implantation. Animal studies were performed in veterinary facilities at The University of Texas M. D. Anderson Cancer Center (Houston, TX), in accordance with institutional guidelines.

Immunohistochemical Analysis

Paraffin-embedded sections of mouse brain tumor were deparaffinized, rehydrated, and equilibrated in PBS. After antigen retrieval, the slides were incubated with 0.3% H_2O_2 in methanol for 30 minutes to quench endogenous peroxidase activity. Then, blocked sections were incubated overnight at 4°C with the following primary antibodies: anti–proliferating cell nuclear antigen (PCNA) (PC-10, diluted 1:500; Dako Co., Carpinteria, CA), anti–smooth muscle actin (SMA) (IA4, diluted 1:500; Dako Co.), anti–von Willebrand factor (factor VIII–related antigen; clone mo812, diluted 1:500; Dako Co.), anti-nestin (MAB353, diluted 1:100; Chemicon, Temecula, CA), and anti-Ang2 (N-18, diluted 1:200; Santa Cruz Biotechnology, Santa Cruz, CA). All slides were subsequently washed for 5 minutes in PBS with 0.1% Tween-20 and incubated with secondary antibodies for 30 minutes. Bound antibodies were detected by the avidin–biotin–peroxidase method with an ABC Elite kit (Vector Laboratories, Burlingame, CA). Staining was performed with diaminobenzidine Stable DAB (Research Genetics, Carlsbad, CA) or Stable Fast red (Research Genetics). Sections were counterstained with hematoxylin (Sigma Chemical Co., St. Louis, MO) and mounted under glass coverslips with Immu-mount (ThermoShandon, Pittsburgh, PA). For factor VIII/nestin immunofluorescence double staining, blocked sections were incubated with anti–factor VIII and anti-nestin antibodies overnight at 4°C and then with secondary Texas red–conjugated antibody (T-2767; Molecular Probes, Eugene, OR) or fluorescein isothiocyanate (FITC)–conjugated antibody (F-2761; Molecular Probes) for 1 hour at room temperature. After washing, mounted slides were analyzed by fluorescent microscopy (Zeiss Axiovert 200; Carl Zeiss MicroImaging, Inc., Thornwood, NY), with separate filters used for each fluorochrome. Images were obtained using the software package XCAP-Lite, Version 2.1 (EPIX, Inc., Buffalo Grove, IL).

Quantification of Microvessel Density (MVD)

Areas containing the most microvessels (or tumor "hot spots") were identified by examining the sections with a light microscope at low magnification (original magnification, ×40 and ×100), as previously described [5,19]. Then, the individually stained microvessels in these areas were counted at ×200 magnification over a square grid that corresponded to a field size of 0.5 mm^2. Large microvessels and single brown-stained endothelial cells that were clearly separate from the microvessels were included in the microvessel count; branching structures were counted as one vessel, unless there was a break in the continuity of the vessel, in which case it was counted as two distinct vessels. The mean number of microvessels counted in five fields was used for analyses.

Adenoviral Constructs

To create the Ang2 adenoviral construct, Ang2 cDNA (1504 bp; GenBank accession no. AF 004327) was amplified by reverse transcription–polymerase chain reaction using

the primers 5′-TACTGAAGAAAGAATGTGG-3′ (forward) and 5′-TTAGAAATCTGCTGGTCGG-3′ (backward) from HUVECs. Subsequently, Ang2 cDNA was cloned into an expression cassette (CMV promoter, SV40pA) in the shuttle adenoviral vector, pDE1sp1A (Microbix Biosystems, Toronto, Ontario, Canada). Then, the replication-deficient adenovirus vector containing the human Ang2 cDNA (AdAng2) was constructed and characterized as described previously [20]. AdCMV, an empty adenovirus vector containing only a Cytomegalovirus promoter and a simian virus 40 polyadenylation signal, was used as control [21]. Culture infections were performed as described previously [21].

Western Blot Analysis

U-87 MG cells (2.5×10^5 cells) were seeded in 60-mm dishes. After 1 day, cells were infected with AdCMV or AdAng2 at the indicated multiplicities of infection (MOI) and were incubated for 2 days. Then cells were washed twice, and 2 ml of serum-free medium was added. After 1 day, the conditioned medium was collected, cells were lysed, and 15 μg of secreted proteins or 30 μg of whole-cell lysates was separated by sodium dodecyl sulfate–polyacrylamide gel electrophoresis and electroblotted onto a nitrocellulose membrane. Ang2 expression was determined by immunoblotting with anti-Ang2 antibody (C-20; Santa Cruz Biotechnology). The membranes were developed using an enhanced chemiluminescence reagent (Amersham Corp., Arlington Heights, IL).

Cell Viability Assay

U-87 MG cells were first mock-treated or treated with AdCMV or AdAng2 at an MOI = 100. Three days later, the apoptotic cell population was determined by staining with Annexin V–FITC (BD Biosciences, San Jose, CA) and propidium iodide (PI), as recommended by the manufacturer. Annexin V–FITC–stained and PI-stained cells were quantified with a FACScalibur (BD Biosciences).

Tube Formation Assay

HUVECs (2×10^4) were seeded on Matrigel-coated 96-well plates (50 μl, 10 mg/ml; BD Biosciences) and grown for 16 hours, in conditioned medium collected from U-87 MG cells treated with AdAng2, AdCMV, 0.1% bovine serum albumin (BSA), or recombinant Ang2 (rAng2; 200 and 400 ng/ml; R&D Systems, Minneapolis, MN). Morphologic cellular changes were visualized with a Zeiss Axiovert 200 microscope and photographed at ×100 magnification by XCAP-Lite, Version 2.1 (EPIX, Inc.).

Chorioallontoic Membrane (CAM) of Chick Embryo Assay

CAM assay was performed as described elsewhere [22], with slight modifications. Briefly, fertilized chick eggs (SPAFAS; Charles River Laboratory, Wilmington, MA) were incubated at 37°C and 55% humidity for 7 days. Filter disks (6 mm in diameter) were coated with cortisone acetate in absolute ethanol (3 mg/ml). CAMs were treated locally with filter disks saturated with a solution containing BSA (0.1%) or rAng2 (200 and 400 ng/ml). The filter was placed on the CAM in a region with the lowest density of blood vessels and in the vicinity of a large vessel as a reference point. Angiogenesis was monitored by photographs taken starting 3 days after treatment. Images were captured using an Olympus stereomicroscope (SZx12; Olympus, Melville, NY) and Spot basic software (Diagnostic Instruments, Inc., Sterling Heights, MI).

Statistical Analyses

Experimental results obtained in the CAM assay were statistically evaluated using Fisher's exact test. Survival was assessed by plotting survival curves according to the Kaplan-Meier method, and comparisons were performed using the log-rank test.

Results

Vascular Development and Tumor Kinetics

To delineate the tumor growth and angiogenic kinetics of U-87 MG intracranial xenografts, we performed a time point analysis of this model after implanting those cells into the brain of nude mice. Eight hours after cell implantation, the cells were grouped together, and there was no evidence of modifications to surrounding host vessels (Figure 1*A*). At this time, more than 90% of implanted cells expressed PCNA, indicating that the implanted U-87 MG cells proliferated actively (Figure 1*B*). Twenty-four hours after cell implantation, the cells were still clustered together as a small mass, but with a center displaying signs of cell death compatible with karyorrhexis (data not shown). At this time, we also observed engorged vessels in the normal parenchyma of mice proximal to the tumor. Interestingly, these vessels were positive for SMA, indicating the existence of reactive pericytes (Figure 1*C*). By day 4, the tumors had grown to a mean volume of 0.37 mm^3 and contained an area of central necrosis surrounded by a mass of cells with a very low MVD (Figure 1*D*, Table 1). The vessels in the host parenchyma surrounding the tumor displayed changes in morphology, including an enlarged diameter and a disorganized structure (Figure 1, *E* and *F*). Some of the vessels interacted physically with peripheral tumor cells. This pattern suggests that the mouse vessels had extended into human tumor cells through the process of cooption and/or new branching. Staining for SMA was intense in peritumoral vessels, and the staining pattern highlighted an important alteration in their architecture, showing disorganized structures that were consistent with vessels undergoing remodeling processes (Figure 1, *D* and *E*). On day 6 after implantation, although the tumors were small (a mean of about 1 mm^3), the MVD curve profile was within its exponential phase (Table 1). Twelve days after implantation, the tumors consisted of sphere-like masses of cells (volume, 31 mm^3), along with intratumoral vessels (MVD mean, 37.55 vessels/0.5 mm^2; Table 1, Figure 1*G*). At this time, we did not find large areas of necrosis or foci of necrosis with pseudopalisading. In addition, the vessels were numerous, large, distorted, and SMA-positive (Figure 1, *G* and *H*). Tumor limits were clearly defined, and cancer cells did not exhibit an invasive pattern into host

tissues, as seen earlier. The tumor volume at 20 days after implantation reached around 100 mm^3 (Table 1). At this time, the tumors also exhibited a high mean MVD (62 vessels/0.5 mm^2) plus a highly proliferative pattern without areas of necrosis (Figure 1, *I* and *J*). All mice showed signs of toxicity by day 30, which correlated with the development of an expansive mass, causing extreme brain compression.

Thus, although the U-87 MG intracranial tumors hardly grew initially while they were avascular structures, as soon as 1 day after implantation and definitely by day 4, changes

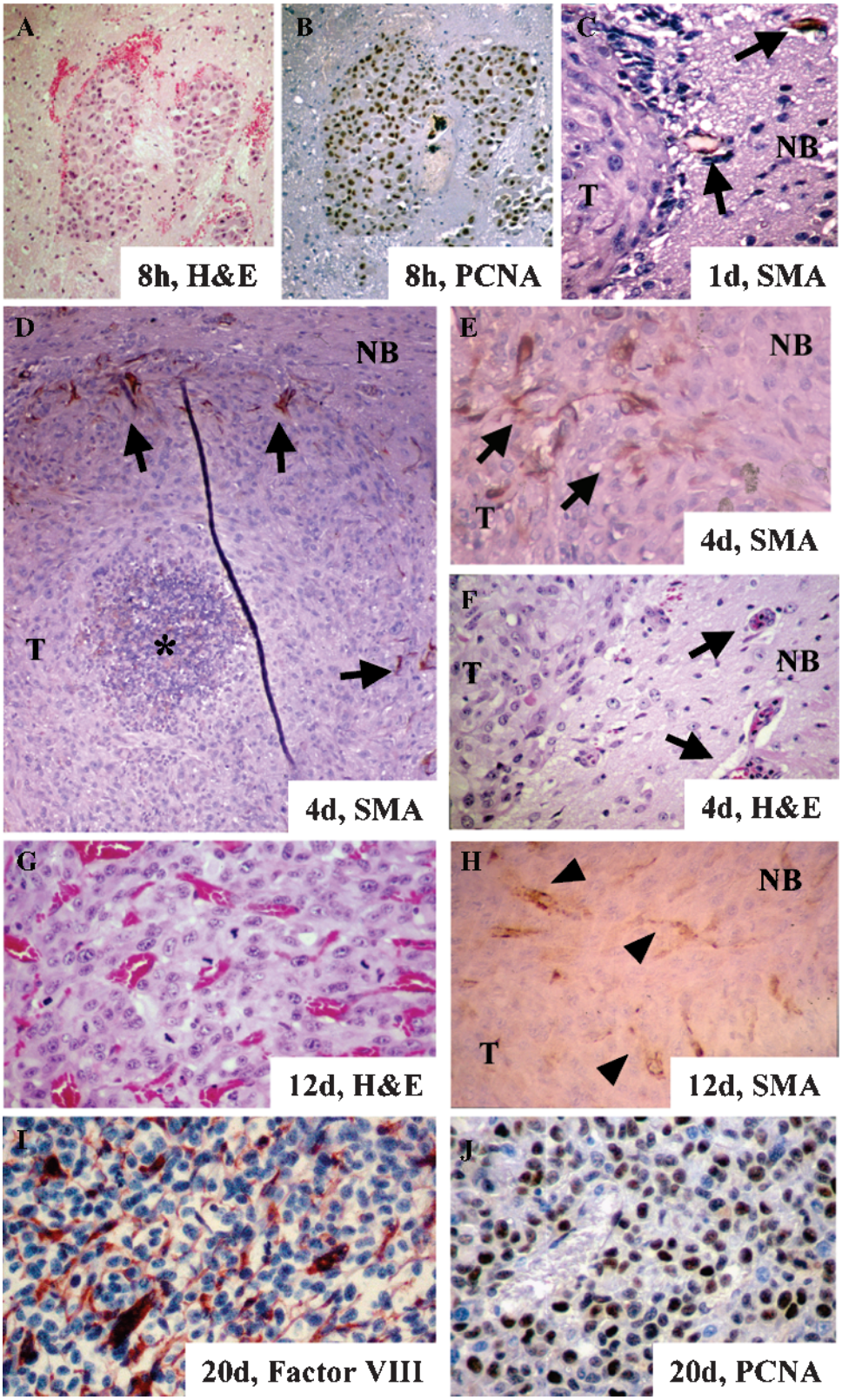

Table 1. Tumor Growth Kinetics and MVD Analyses of U-87 MG Xenografts.

Time after Implantation	*n*	Volume (mm^3)		MVD (vessels/0.5 mm^2)	
		Mean	SD	Mean	SD
8 hr	3	0.03	0.01	0	0
1 day	4	0.04	0.01	0.05	0.10
4 days	4	0.37	0.08	6.65	0.68
6 days	3	1.04	0.17	18.50	3.09
12 days	4	31.06	7.65	37.55	2.68
17 days	3	62.30	5.93	43.20	4.28
20 days	4	99.03	7.74	62.45	7.80

in the host vessels were evident; these included the existence of engorged SMA-positive vascular structures in the periphery of the xenograft. In the case of U-87 MG tumors, this was accompanied by central necrosis that disappeared by 1 week after implantation when intratumoral angiogenesis became evident. After this, increased MVD was associated with exponential tumor growth and with a decrease in induced angiogenesis within the host and in the tumor periphery.

Ang2 Expression Pattern during Glioma Development

Because Ang2 is considered a complex regulator of vascular remodeling, we studied the temporal and spatial expressions of Ang2 during early angiogenesis (before day 4 after cell implantation) and later when intratumoral angiogenesis had become established and peripheral angiogenesis had become weaker (12–20 days after cell implantation). We found that, during the early stage when the host vessels were being coopted, the inner regions of the tumor did not express Ang2. However, Ang2 was highly expressed in the cytoplasm of most glioma cells within the vicinity of normal tissues (Figure 2*A*). This zone of expression of Ang2 was approximately 10 cell layers thick, covered the entire the tumor, and engulfed reactive vascular structures that had developed in the border between the tumor and the normal brain. Positive Ang2 staining was also seen in a few isolated cells in the normal brain zone, suggesting the presence of tumor-infiltrative cells. Weaker Ang2 expression was also observed in the cellular components of the reactive vessels surrounding the tumor (Figure 2*A*). This well-defined distribution of Ang2 expression suggested a role for Ang2 in the cooption of vessels. However, with tumor growth, the pattern of expression of Ang2 changed drastically. Thus, by 11 days after tumor cell implantation, Ang2 expression was dramatically reduced in the tumor cells, such that the tumor had become an Ang2-negative mass. Thus, Ang2 does not seem to be produced in high amounts during the exponential phase of tumor growth. Although we hardly detected Ang2 expression within the vascular component at the center of the tumor, which by now was already well developed, we did observe vascular structures that were weakly positive for Ang2 at the tumor edge (Figure 2, *B* and *C*). These vessels were, in general, enlarged. Collectively, these observations suggest that high Ang2 expression is required during the early stages of tumor development but that Ang2 is downmodulated once the vascular structure of the tumor has been developed.

Because nestin is a marker for proliferative endothelium in gliomas [23], we next examined whether there was temporal and spatial parallelism in the expression of nestin and Ang2. First, we confirmed that nestin was expressed in tumoral vessels in the U-87 MG xenograft model. In these experiments, we performed double immunofluorescence for factor VIII and nestin in a 20-day xenograft. As expected, most of the vascular structures identified with phase-contrast studies were positive for both markers (Figure 2, *D* and *E*). Then, we examined the expression of nestin during U-87 MG tumor development. In the early angiogenic phase, nestin was clearly expressed in vascular structures surrounding the tumor (Figure 2*F*). In fact, nestin expression was more evident and frequent in vascular structures at this time of tumor development than was Ang2. Although nestin was also detected in scattered glioma cells, it assumed no specific pattern and in no way assumed the ring-like distribution seen for Ang2 in the tumor. Therefore, in the early stages of tumor development, nestin expression was more intense in the vessels than in the glioma cells; therefore, it did not completely colocalize with Ang2. The differences in the expression between the two proteins were more marked in the late stages of tumor development. Thus, although Ang2 expression in the glial or the vascular component of the tumor faded in the late stages of tumor development (> 11 days after cell implantation), nestin was widely expressed in intratumoral vessels and in scattered cancer cells (Figure 2*G*).

Together, our results showed that Ang2 is overexpressed early in angiogenesis, not only in vascular structures [7,8,24,25] but also in the tumor cells, specifically in the periphery, where vascular cooption takes place. Furthermore, our finding that Ang2 and nestin expressions are not correlated in advanced tumors could indicate that, although

Figure 1. *Vascular development of the U-87 MG intracranial animal model. Examination of implanted U-87 MG cells at different time points of tumor growth. (A and B) A group of U-87 MG tumor cells 8 hours after implantation in an H&E–stained section (A) and in a PCNA-immunostained section (B) showing proliferation (PCNA-positive, DAB staining; original magnification, ×100). (C) Implanted cells on day 1. Note the incipient hyperplasia of vessels near the tumor interface that stained positive for SMA (arrows) (DAB staining; original magnification, ×400). (D–F) U-87 intracranial xenograft on day 4 after implantation. A central area of necrosis (indicated by asterisk) and SMA-immunoreactive host vessels establishing intimate contact in the periphery of the tumor. Note the highly disorganized structure (arrows in D) (DAB staining; original magnification, ×100). In a close-up view of the tumor/normal brain interface, we observed numerous SMA-positive hypervascular structures (arrows in E) (DAB staining; original magnification, ×400). (F) Note the presence of reactive vessels (arrows) from the host near the tumor and in the tumor periphery (H&E; original magnification, ×400). (G and H) U-87 MG xenograft on day 12. (G) H&E–stained section showing high microvascular density with engorged structures (original magnification, ×400). (H) Intratumoral vessels (arrowheads) that were positive for anti-SMA antibody (DAB staining; original magnification, ×400). (I and J) U-87 MG xenograft 20 days after cell implantation. (I) Staining with anti–factor VIII antibody showed a highly vascularized tumor (Stable Fast red staining; original magnification, ×400) (J) PCNA immunoreactivity was seen in most of the neoplastic glial cells (DAB staining; original magnification, ×400). T, tumor; NB, normal brain.*

some proliferative endothelial events occur in vessels at this stage, Ang2-mediated activity is not required or needs to be downmodulated for a stabilized intratumoral vascular network to be maintained.

Ang2 Induces the Regression of Tubular Structures of Vessels In Vitro

Based on the bimodal pattern of expression of Ang2 during U-87 MG tumor development, we hypothesized that modifying the Ang2 expression profile would impair vascularization and subsequent tumor growth. To test this possibility, we first constructed a replication-deficient adenovirus carrying the full-length wild-type Ang2 cDNA, AdAng2. We then tested the efficacy of this vector in transducing Ang2 by treating U-87 MG cells with AdAng2 at different doses and then by performing Western blot analysis to determine the expression of Ang2 in both the whole-cell lysate and the conditioned medium. This showed that exogenous Ang2 was expressed in a dose-dependent fashion and was secreted into the extracellular milieu, mimicking the trafficking of the endogenous protein (Figure 3*A*) without significantly modifying the viability of the cultures (Figure 3*B*).

To investigate the effect of Ang2 overexpression on vessel formation, we first performed an *in vitro* tube formation assay. HUVECs cultured on Matrigel formed tube-like structures within 16 hours. When endothelial cells were exposed to conditioned media from AdAng2-treated U-87 MG cells, we observed the production of foreshortened and severely broken tubes (Figure 3*C*). Of importance, these findings were similar to those for HUVECs exposed to rAng2 (200 and 400 ng/ml). As expected, as with untreated cells, HUVECs exposed to the conditioned media from U-87 MG cells treated with AdCMV or BSA formed tube-like structures within 16 hours of treatment.

Ang2 Impairs Angiogenesis In Vivo

Using a CAM chicken model system, we next assessed whether the Ang2-induced modifications of the phenotype of endothelial cells interfered with angiogenesis *in vivo*. This showed that Ang2 dramatically decreased newly sprouting angiogenic vessels and caused them to assume a "branchless" pattern by 72 hours of treatment without any signs of hemorrhage and with no egg lethality (Figure 3*D*). In particular, angiogenesis was impaired in 73.3% and 76.9% of Ang2-treated CAMs at a dose of 200 and 400 ng/ml, respectively (Figure 3*D*). Together, our *in vitro* and *in vivo* results showed that, when Ang2 expression is sustained, Ang2 acts as an antiangiogenic molecule by disturbing the necessary organization of endothelial cells such that new branches cannot form during angiogenesis. Moreover, the fact that no signs of hemorrhage were observed indicates that the overexpression of Ang2 does not result in detectable disruption of already formed vessels.

Sustained Expression of Ang2 Induces Tumor Inhibition

We next examined the effects of sustained Ang2 expression on pre-established intracranial glioma xenografts. Thus, animals were treated with intratumoral injections of

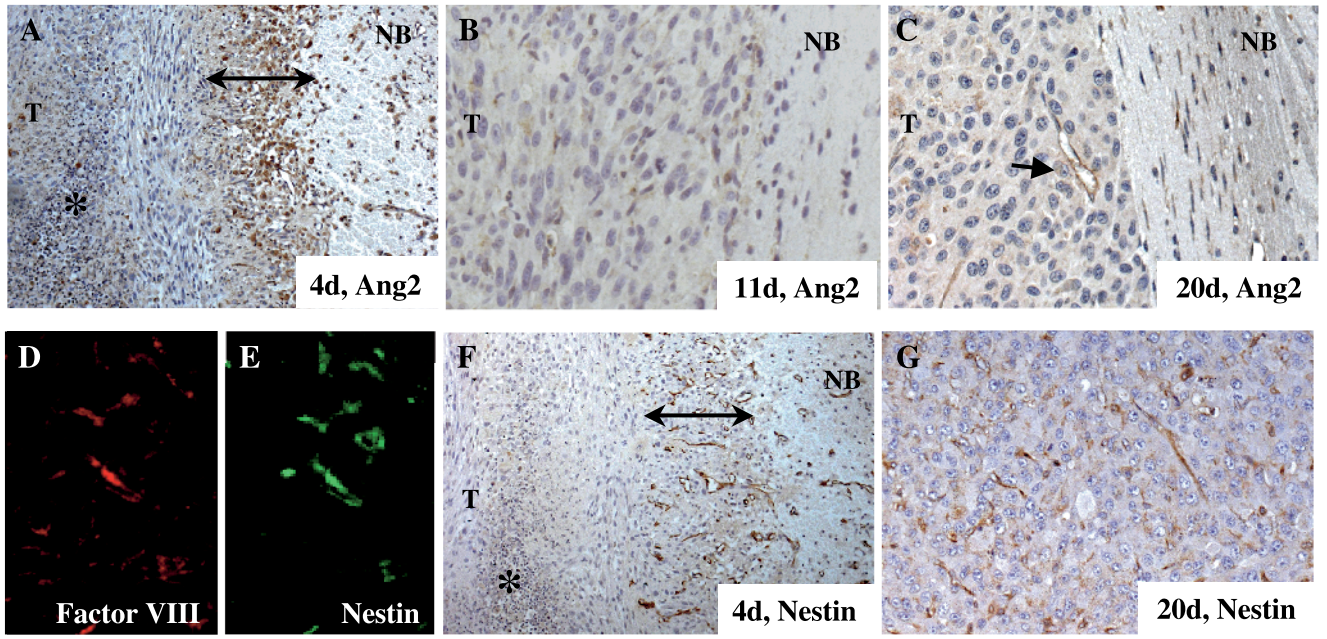

Figure 2. *Expression pattern of Ang2 and nestin during U-87 MG xenograft development. (A–C) Ang2 expression in U-87 MG intracranial xenografts on day 4 (A), day 11 (B), and day 20 (C) after cell implantation. At an early time point, Ang2 was overexpressed in glial cells at the tumoral edge (double-headed arrow) and in vascular structures (arrows) in the tumor/normal brain interface (DAB staining; original magnification, ×100). However, on days 11 and 20, Ang2 expression was detectable mainly in some vessels (arrows) in the periphery of the tumor (DAB staining; original magnification, ×400). (D and E) Double immunofluorescence studies using anti–factor VIII and anti-nestin antibodies indicate that nestin is expressed in vascular structures on day 20 after implantation (original magnification, ×400). (F and G) Nestin expression in U-87 MG intracranial xenografts on day 4 (F) and day 20 (G) after cell implantation. Nestin is overexpressed in host vessels at the tumoral edge (double-headed arrow) and in host vessels during early intense angiogenesis (DAB staining; original magnification, ×100). After vessel cooption, nestin is expressed by intratumoral vessels (DAB staining; original magnification, ×400). T, tumor; NB, normal brain.*

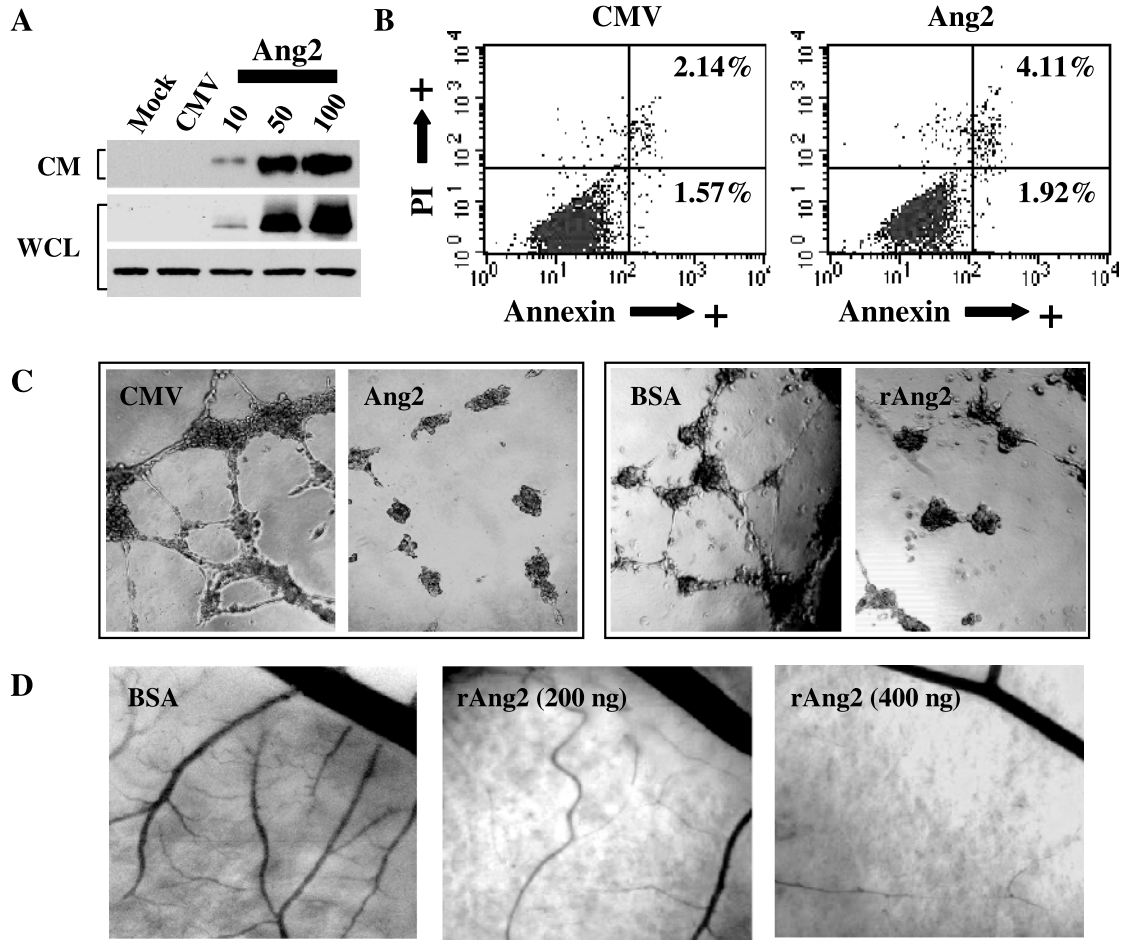

	BSA	Ang2 *(200 ng)*	Ang2 *(400 ng)*
Total samples tested (*n*)	**25**	**15**	**26**
Impaired angiogenesis (*n*)	**4**	**11**	**20**
***P* value**		**0.0005**	**<0.0001**

Figure 3. *Ang2 inhibits angiogenesis in vitro and in vivo. (A) Transduction efficiency of AdAng2. As shown by Western blot analysis, exogenous Ang2 was expressed in a dose-dependent manner in both the whole-cell lysate (WCL) and the conditioned medium (CM) of Ang2-treated U-87 MG cells. Actin expression was used as loading control. (B) Viability analysis of AdAng2-treated U-87 MG cells. Apoptotic populations of U-87 MG cells were quantified 3 days after infection with AdAng2 or AdCMV (MOI = 100) by Annexin V and PI staining and by FACS analysis. The percentages of cells in the early stage [Annexin V (+)/PI (−)] and in the late stage of apoptosis or cell death [Annexin V (+)/PI (+)] are shown. (C) Inhibition of tube formation of endothelial cells by Ang2. HUVECs plated in Matrigel-coated dishes were incubated with the conditioned medium from U-87 MG cells previously treated with AdAng2 (Ang2), AdCMV (CMV), rAng2 (400 ng/ml), or BSA (as control) (MOI = 100). Ang2 expression resulted in drastically disrupted capillary-like structures in vitro. Micrographs of typical fields illustrate HUVEC tube formation under the influence of several different treatments. (D) Inhibitory effect of Ang2 on the capillary plexus of a CAM system. En face images of developing CAMs treated with filter disks coated with BSA (0.1%) or Ang2 (200 or 400 ng/ml). Normal vascular distribution was observed in CAMs treated with BSA. Ang2 diminished the capillary network. This Ang2-mediated inhibition of angiogenesis in the CAM assay was quantified in terms of the total number of eggs and the number of eggs that exhibited inhibition of angiogenesis (table in the figure). For the comparison of Ang2-treated CAMs and control-treated CAMs, P values were determined by Fisher's exact test.*

AdAng2, AdCMV, or PBS starting on day 4 after cell implantation. The median survival was 28 to 29 days in the control groups, and all these animals died by day 32. In contrast, treatment with AdAng2 significantly prolonged the survival of U-87 MG tumor–bearing animals (median overall survival, 48 days) compared with control-treated animals ($P = .0003$; Figure 4*A*).

To determine the antitumoral effects of Ang2, we sacrificed two animals in every group 10 days after cell implantation. At that time, as expected, the brains of control animals with adenoviral vector–treated glioma xenografts showed hypercellular, highly vascularized tumors with no areas of necrosis. There was also a developed vascular network, predominantly near the tumor interface, as shown by immunostaining using

anti–factor VIII antibody (Figure 4*B*). In AdAng2-treated xenografts, however, we observed large areas of necrosis, karyorrhexis, and vascular damage, as revealed by varying degrees of fibrinoid necrosis. Vascular fibrinoid necrosis was more predominant at the center of the tumor, corresponding to the most intense areas of tumor necrosis (Figure 4*B*). Factor VIII staining also showed a disorganized vascular network in the periphery of the tumor, in conjunction with extensive avascular areas (Figure 4*B*). These data were in accordance with the findings from the *in vitro* tube formation assay and the CAM model experiments, thus collectively indicating that the induction and successful branching of blood vessels were largely inhibited in the tumor interface region of Ang2-treated tumors.

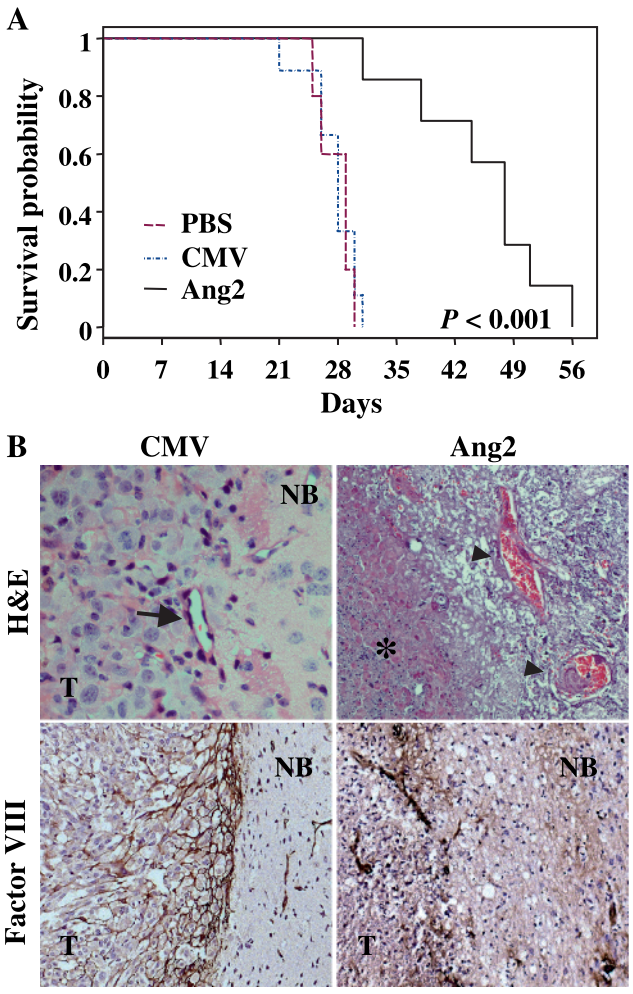

Figure 4. *The sustained expression of Ang2 prolongs the survival of human glioma–bearing animals. (A) Kaplan-Meier survival curves of nude mice bearing U-87 MG intracranial xenografts treated (3 days after cell implantation) with AdAng2 (Ang2), AdCMV (CMV), or PBS (twice a week for a total of 3 weeks) using a guide-screw system. P values were determined by means of a log rank test and represent survival comparisons of AdAng2-treated mice and AdCMV-treated mice. (B) High-magnification cross-sectional views of H&E–stained sections of AdAng2- and AdCMV-treated intracranial tumors 10 days after cell implantation (upper panel, arrow) (original magnification, ×400; note the structure of the vessel within the tumor). Extensive areas of necrosis were found in both tumor cells (karyorrhexis; asterisk) and vessels within the tumor (fibrinoid hyalinosis; arrowheads) in the Ang2-treated xenografts. Factor VIII staining revealed disruption of the vascular network and extensive avascular areas in the tumor/normal brain interface of Ang2-treated mice (bottom panel) (original magnification, ×100). T, tumor; NB, normal brain.*

Discussion

Our analysis of angiogenesis and the growth characteristics of U-87 MG human glioma xenografts intracranially implanted in nude mice showed that angiogenesis was accomplished in a stepwise fashion, consisting first of vessel development and then of intratumoral vessel network maintenance. One particularly notable finding was the observation that Ang2 expression is detected not only in vascular structures but also in glioma cells. This observable fact happens early in tumor development, and its expression is downmodulated and largely restricted to vascular structures during the vascular phase of tumor growth, which suggests that the sustained expression of Ang2 might serve as an antitumor strategy. As a proof of principle of this possible effect of Ang2 on this model, we treated U-87 MG tumors with Ang2 during the intermediate and advanced stages of vascular formation. This modification in the pattern of Ang2 expression induced vascular instability and inhibited tumor growth, which resulted in the prolonged survival of U-87 MG–bearing animals.

Currently there are several well-characterized syngeneic models of gliomas. Of these, the most frequently used are the rat C6 [7] and mouse GL261 [8] models. Similar to the nonsyngeneic U-87 MG model that we studied here, tumor growth in these models results in the death of animals from a mass effect, and disease progression is highly reproducible [17]. However, these models differ from the U-87 MG model in several ways (Figure 5). One is that the C6 and GL261 tumors start off as parasitic small tumors around pre-existing vessels, although the cooption of host tissue vessels is also observed [7,8,26]. Robust angiogenesis develops within days in the U-87 MG model, and within weeks in the C6 and GL261 models. Therefore, it would seem that angiogenesis is more effective in the U-87 MG model than in the rodent models, circumventing the noteworthy hypoxia and necrosis that occur concomitantly with vessel regression in the C6 and GL261 models. Although the models discussed here seem to differ partially in regard to the chronology of angiogenesis and the temporal and spatial expressions of Ang2, a similar rationale for the observed pattern of Ang2 expression applies to all, in that the expression of Ang2 precedes or coincides with tumor necrosis and vascular remodeling. Thus, in the U-87 MG model, Ang2 is expressed in the vicinity of normal tissues during the early vascular (cooption phase) stage of the tumor. The expression of Ang2 at this time could allow for vascular destabilization and remodeling [7,8], leading to the branching of host vessels, which allows them to infiltrate the incipient tumor mass. Later low levels of Ang2 expression in the U-87 MG model are consistent with the lack of tumoral necrosis resulting from devastating vessel regression and with a decrease in peripheral angiogenesis. The genetic dissimilarity between human and rodent cancer cells, as well as the different cross-talk signaling between rodent–rodent and rodent–human tissues, might help explain partially the

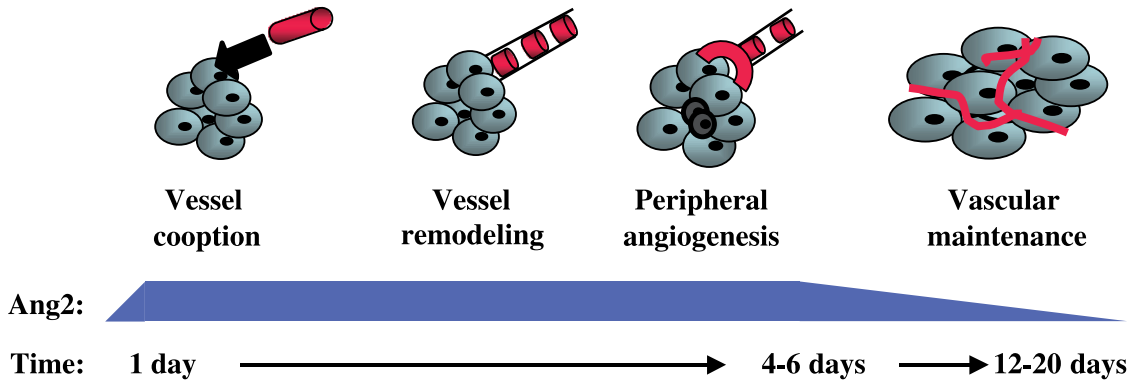

Figure 5. *Schematic representation of the multistage nature of tumoral angiogenesis in the U-87 MG intracranial model. The U-87 MG growth pattern is characterized by early vessel (red structures) cooption, with signs of vascular destabilization followed by remodeling (represented as dotted red structures), which will finally lead to florid peripheral angiogenesis within 10 days after cell implantation. Initial and transitory central necrosis is represented by small darker cells. Note that the level of expression of Ang2 coincides with vessel remodeling and initiation of peripheral angiogenesis. Downmodulation of Ang2 levels, along with high tumoral microvascular density, is observed in later stages.*

differences in the chronology of angiogenesis seen among animal models.

Several reports support the expression of Ang2 as a unique feature of vascular structures [7,8,24,25]. Nonetheless, our findings are consistent with those of others, wherein the expression of Ang2 is observed also in cancer cells [27,28]. The high expression of Ang2 by the neoplastic glial compartment of U-87 MG xenografts, specifically in the periphery of the tumor, suggests at least a paracrine function for Ang2 in the regulation of initial angiogenesis, which could be unnecessary or even disadvantageous in the latter stages of vascular maintenance.

Based on our hypothesis that the sustained expression of Ang2 could promote vessel involution and tumor necrosis, we developed a novel therapeutic strategy that would maintain high intratumoral levels of Ang2 throughout the evolution of U-87 MG xenografts. Our data indicated that the resultant sustained expression of Ang2 inhibited tumor growth due, at least, to impaired vascularization. These data were confirmed by our data from the tube formation assay and the CAM chicken embryo assay. Moreover, these results dramatically buttress the belief that Ang2 expression in the intermediate phases of the C6 and GL216 models is responsible for vessel involution [7,8]. In line with this, Machein et al. [16] reported recently that the implantation of Ang2-transfected mouse cells into the brains of animals resulted in smaller tumors with aberrant vascularity. Strong evidence supporting the antiangiogenic role of Ang2 also comes from Ang2-overexpressing transgenic animal models, which showed widespread vessel discontinuity and embryonic lethality [12]. However, another study in which an intracranial animal model was used showed that glioma cells overexpressing Ang2 displayed an invasive phenotype [15]. It is certainly possible that different relative levels of Ang2 could lead to very different outcomes, as suggested in previous descriptive reports and by studies in transgenic mice in which the expression of Ang2 and/or vascular endothelial growth factor was induced in the choroidal and retinal circulations [29,30]. This varying expression threshold might explain the different results obtained for the clonal selection of cells expressing Ang2 [15].

In summary, we have identified the chronology of angiogenesis and Ang2 expression in the commonly used U-87 MG model. Our data indicate that angiogenesis in the U-87 MG model differs from that in the syngeneic C6 and GL261 glioma models. We also showed that continuous expression of Ang2 results in vessel disorganization and inadequate angiogenesis, hence inhibiting tumor growth. Before Ang2-based antiglioma therapies are implemented, studies should be performed to further clarify the controversial role of Ang2 in tumor angiogenesis and invasion.

Acknowledgements

We are much indebted to Betty L. Notzon (Department of Scientific Publications, The University of Texas M. D. Anderson Cancer Center) for editorial assistance, and to Joy Gumin and Verlene Henry (Brain Tumor Center, The University of Texas M. D. Anderson Cancer Center) for excellent technical support.

References

[1] Levin VA, Gutin PH, and Leivel S (1997). Neoplasms of the central nervous system. In *Cancer. Principles and Practice of Oncology* (5th ed). DeVita VT, Hellman SJ, Rosenberg SA, (Eds). Philadelphia, PA, pp. 2022–2072.

[2] Maher EA, Furnari FB, Bachoo RM, Rowitch DH, Louis DN, Cavenee WK, and DePinho RA (2001). Malignant glioma: genetics and biology of a grave matter. *Genes Dev* **15,** 1311–1333.

[3] Hanahan D and Folkman J (1996). Patterns and emerging mechanisms of the angiogenic switch during tumorigenesis. *Cell* **86,** 353–364.

[4] Hlatky L, Hahnfeldt P, and Folkman J (2002). Clinical application of antiangiogenic therapy: microvessel density, what it does and doesn't tell us. *J Natl Cancer Inst* **94,** 883–893.

[5] Weidner N, Semple JP, Welch WR, and Folkman J (1991). Tumor angiogenesis and metastasis—correlation in invasive breast carcinoma. *N Engl J Med* **324,** 1–8.

[6] Bergers G, Javaherian K, Lo KM, Folkman J, and Hanahan D (1999). Effects of angiogenesis inhibitors on multistage carcinogenesis in mice. *Science* **284,** 808–812.

[7] Holash J, Maisonpierre PC, Compton D, Boland P, Alexander CR, Zagzag D, Yancopoulos GD, and Wiegand SJ (1999). Vessel cooption,

regression, and growth in tumors mediated by angiopoietins and VEGF. *Science* **284,** 1994–1998.

[8] Zagzag D, Amirnovin R, Greco MA, Yee H, Holash J, Wiegand SJ, Zabski S, Yancopoulos GD, and Grumet M (2000). Vascular apoptosis and involution in gliomas precede neovascularization: a novel concept for glioma growth and angiogenesis. *Lab Invest* **80,** 837–849.

[9] D'Angelo MG, Afanasieva DA, and Aguzzi T (2000). Angiogenesis in transgenic models of multistep carcinogenesis. *J Neuro-Oncol* **50,** 89–98.

[10] Bergers G and Benjamin LE (2003). Tumorigenesis and the angiogenic switch. *Nat Rev Cancer* **3,** 401–410.

[11] Goldbrunner RH, Wagner S, Roosen K, and Tonn JC (2000). Models for assessment of angiogenesis in gliomas. *J Neuro-Oncol* **50,** 53–62.

[12] Maisonpierre PC, Suri C, Jones PF, Bartunkova S, Wiegand SJ, Radziejewski C, Compton D, McClain J, Aldrich TH, Papadopoulos N, et al. (1997). Angiopoietin-2, a natural antagonist for Tie2 that disrupts *in vivo* angiogenesis. *Science* **277,** 55–60.

[13] Goede V, Schmidt T, Kimmina S, Kozian D, and Augustin HG (1998). Analysis of blood vessel maturation processes during cyclic ovarian angiogenesis. *Lab Invest* **78,** 1385–1394.

[14] Gale NW, Thurston G, Hackett SF, Renard R, Wang Q, McClain J, Martin C, Witte C, Witte MH, Jackson D, et al. (2002). Angiopoietin-2 is required for postnatal angiogenesis and lymphatic patterning, and only the latter role is rescued by Angiopoietin-1. *Dev Cell* **3,** 411–423.

[15] Hu B, Guo P, Fang Q, Tao HQ, Wang D, Nagane M, Huang HJ, Gunji Y, Nishikawa R, Alitalo K, et al. (2003). Angiopoietin-2 induces human glioma invasion through the activation of matrix metalloprotease-2. *Proc Natl Acad Sci USA* **100,** 8904–8909.

[16] Machein MR, Knedla A, Knoth R, Wagner S, Neuschl E, and Plate KH (2004). Angiopoietin-1 promotes tumor angiogenesis in a rat glioma model. *Am J Pathol* **165,** 1557–1570.

[17] Lal S, Lacroix M, Tofilon P, Fuller GN, Sawaya R, and Lang FF (2000). An implantable guide-screw system for brain tumor studies in small animals. *J Neurosurg* **92,** 326–333.

[18] Attia MA and Weiss DW (1966). Immunology of spontaneous mammary carcinomas in mice: V. Acquired tumor resistance and enhancement in strain A mice infected with mammary tumor virus. *Cancer Res* **26,** 1787–1800.

[19] Im SA, Kim JS, Gomez-Manzano C, Fueyo J, Liu TJ, Cho MS, Seong CM, Lee SN, Hong YK, and Yung WK (2001). Inhibition of breast cancer growth *in vivo* by antiangiogenesis gene therapy with adenovirus-mediated antisense-VEGF. *Br J Cancer* **84,** 1252–1257.

[20] Fueyo J, Gomez-Manzano C, Yung WK, Liu TJ, Alemany R, Bruner JM, Chintala SK, Rao JS, Levin VA, and Kyritsis AP (1998). Suppression of human glioma growth by adenovirus-mediated *Rb* gene transfer. *Neurology* **50,** 1307–1315.

[21] Gomez-Manzano C, Fueyo J, Kyritsis AP, McDonnell TJ, Steck PA, Levin VA, and Yung WK (1997). Characterization of p53 and p21 functional interactions in glioma cells en route to apoptosis. *J Natl Cancer Inst* **89,** 1036–1044.

[22] Brooks PC, Montgomery AM, and Cheresh DA (1999). Use of the 10-day-old chick embryo model for studying angiogenesis. *Methods Mol Biol* **129,** 257–269.

[23] Sugawara K, Kurihara H, Negishi M, Saito N, Nakazato Y, Sasaki T, and Takeuchi T (2002). Nestin as a marker for proliferative endothelium in gliomas. *Lab Invest* **82,** 345–351.

[24] Zagzag D, Hooper A, Friedlander DR, Chan W, Holash J, Wiegand SJ, Yancopoulos GD, and Grumet M (1999). *In situ* expression of angiopoietins in astrocytomas identifies angiopoietin-2 as an early marker of tumor angiogenesis. *Exp Neurol* **159,** 391–400.

[25] Stratmann A, Risau W, and Plate KH (1998). Cell type–specific expression of angiopoietin-1 and angiopoietin-2 suggests a role in glioblastoma angiogenesis. *Am J Pathol* **153,** 1459–1466.

[26] Nagano N, Sasaki H, Aoyagi M, and Hirakawa K (1993). Invasion of experimental rat brain tumor: early morphological changes following microinjection of C6 glioma cells. *Acta Neuropathol (Berl)* **86,** 117–125.

[27] Koga K, Todaka T, Morioka M, Hamada J, Kai Y, Yano S, Okamura A, Takakura N, Suda T, and Ushio Y (2001). Expression of angiopoietin-2 in human glioma cells and its role for angiogenesis. *Cancer Res* **61,** 6248–6254.

[28] Zadeh G and Guha A (2003). Neoangiogenesis in human astrocytomas: expression and functional role of angiopoietins and their cognate receptors. *Front Biosci* **8,** e128–e137.

[29] Yancopoulos GD, Davis S, Gale NW, Rudge JS, Wiegand SJ, and Holash J (2000). Vascular-specific growth factors and blood vessel formation. *Nature* **407,** 242–248.

[30] Oshima Y, Oshima S, Nambu H, Kachi S, Takahashi K, Umeda N, Shen J, Dong A, Apte RS, Duh E, et al. (2005). Different effects of angiopoietin-2 in different vascular beds: new vessels are most sensitive. *FASEB J* **19,** 963–965.